Bell-Type Test of Energy-Time Entangled Qutrits

R. T. Thew,[1,*] A. Acín,[1,2] H. Zbinden,[1] and N. Gisin[1]

[1]*Group of Applied Physics, University of Geneva, 1211 Geneva 4, Switzerland*
[2]*Institut de Ciències Fotòniques, Jordi Girona 29, 08034 Barcelona, Spain*
(Received 9 February 2004; published 2 July 2004)

We have performed a Bell-type test for energy-time entangled qutrits. A method of inferring the Bell violation in terms of an associated interference visibility is derived. Using this scheme we obtained a Bell value of 2.784 ± 0.023, representing a violation of 34σ above the limit for local variables. The scheme has been developed for use at telecom wavelengths and using proven long distance quantum communication architecture to optimize the utility of this high dimensional entanglement resource.

Bell inequalities [1] and other tests of nonlocality [2] have a rich history in the evolution and understanding of quantum correlations and, more specifically, entanglement. This grew out of the EPR position on the completeness of quantum mechanics [3]. However, more recently, we have been able to approach these tests from another perspective—that the violation of one of these Bell-type inequalities can be seen as a witness of *useful* entanglement [4]. This has its roots in the qubit domain but has also been extended to qutrits, $d = 3$ dimensional systems, in the context of quantum complexity [5]. This is just one example of the current trend towards investigating higher-dimensional entanglement. This trend is motivated primarily by the promise of improved robustness of these states to noise and the possibility of increased transmission rates for quantum key distribution schemes [6–8]. Perhaps more interestingly, however, is that with the increased complexity of these higher-dimensional states comes the possibility of new quantum protocols that can capitalize on this useful entanglement.

There have been significant advances recently in the experimental investigation of higher-dimensional entanglement. A range of schemes using various degrees of freedom have been put forth: a four-photon polarization scheme generating states with spin-1 statistics [9] and a scheme incorporating lower order modes of orbital angular momentum (OAM) for photons producing qutrits [10] have both performed Bell-type tests; quantum state tomography has recently been performed for OAM entangled qutrits [11] and interference experiments have shown time-bin entanglement up to $d = 20$ [12].

Photonic entanglement is, however, best suited for quantum communication; therefore if we are going to perform any protocol or distribute any entanglement over significant distance, we need to think about the architecture we use. A four-photon scheme, apart from obvious constraints due to polarization, is impractical as the encoding relies on all four photons being transmitted and detected. The OAM scheme will again have problems with long distance fiber transmission predominantly due to dispersive effects between the different modes. By contrast, energy-time, and the similar time-bin, entanglement have a proven history over a long distance [13–15] and the qutrit is encoded on a single photon.

In this Letter, we present the results for a Bell-type test, based on the inequality of Collins *et al.* [16] (CGLMP-Bell), for energy-time entangled qutrits. The scheme is a natural extension of the Franson arrangement for qubits [17], and indeed the idea has previously been proposed [18]. We also introduce a method and the associated constraints one needs to infer a Bell violation from an interference visibility. We discuss how these constraints correspond to the perception that higher-dimensional entanglement is more robust and what this implies experimentally.

We will detail our approach to performing a Bell test momentarily, but first let us remind ourselves of the basic plot. In theory, the Bell test begins with the usual suspects, two parties: Alice and Bob, who are spatially separated. They share a maximally entangled qutrit state and they can choose between two different measurements of three outcomes. They determine various probabilities for the different measurements and outcomes and calculate the relevant function to test the inequality.

First, we consider the experimental setup used to perform this Bell test (see the schematic of Fig. 1) to motivate a physical interpretation when we introduce the inequality. We use energy-time entangled photon pairs created at telecom wavelengths, via a periodically poled lithium niobate (PPLN) waveguide [19], and two three-arm interferometers [20] to generate and analyze entangled qutrits. For each interferometer, we can define a phase vector consisting of the two independent phases, e.g., the relative phases between the short-medium (m) and short-long (l), path lengths. Coincidence measurements at the outputs of the interferometers project onto entangled qutrit states defined when the photons take the same path in each interferometer, short-short or medium-medium or long-long at Alice-Bob.

For energy-time entanglement, this is realized by imagining that we have some detection time, say, $t_0 + t_A$ for Alice, where t_A is the optical distance from the photon
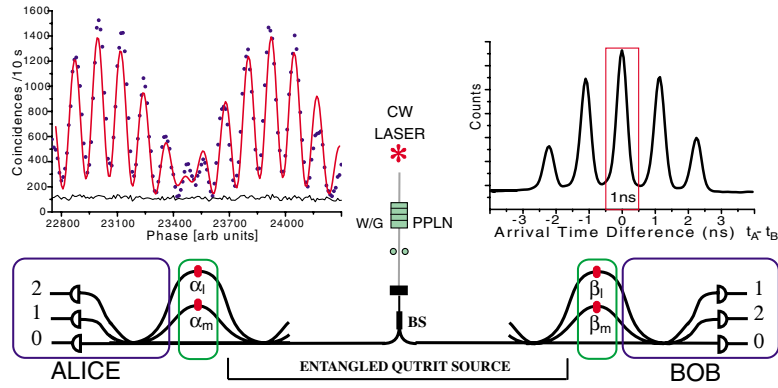
FIG. 1 (color online). Alice and Bob share entangled (energy time at 1300 nm) qutrits. Measurements are determined via variations in the path lengths of their interferometers. There are five peaks in the arrival time histogram (shown on the right) due to different path combinations. Coincidence detection events in the central peak project onto one of three orthogonal entangled qutrit states. These coincidences (shown on the left) vary as a function of Alice and Bob's phase vectors.

pair source to the detector, and a similar time for Bob. Because of the long coherence length of the cw laser, we do not have a well-defined t_0. However, with the hindsight of postselection we can define a coherent superposition of three time-bin amplitudes, t_0, $t_0 - \Delta\tau$, $t_0 - 2\Delta\tau$, relative to the source that have well-defined time differences. Thus, we have our qutrit state prepared. Passing through the interferometer allows one to vary the two relative phases between these time bins. As the path-length differences in the interferometer are $\Delta\tau$ and $2\Delta\tau$, exiting the interferometer corresponds to a Fourier transform and a measurement in the transform basis defined by the postselected t_0. Bob does the same for his $t_0 + t_B$, and we postselect entangled qutrits. (The histogram central peak is centered at $t_B - t_A = 0$.)

An arrival-time-difference histogram with five peaks, due to all the possible path combinations, similar to the inset on the right of Fig. 1, is generated for each detector combination. Coincidence events in these central peaks correspond to projections onto states of the form

$$|\psi(j, k)\rangle \propto c_s|ss\rangle + c_m e^{i(\alpha_m + \beta_m + \phi_{jk}^m)}|mm\rangle$$
$$+ c_l e^{i(\alpha_l + \beta_l + \phi_{jk}^l)}|ll\rangle. \qquad (1)$$

Here α_m, α_l and β_m, β_l, represent the phases in Alice and Bob's medium and long interferometer arms. ϕ_{jk}^m and ϕ_{jk}^l are multiples of $2\pi/3$ which depend on the path taken by the photons in the interferometer and which output, $j, k \in \{0, 1, 2\}_{A,B}$, they take [21,22].

To have maximally entangled qutrits we need $|c_s|^2 = |c_m|^2 = |c_l|^2$. Experimentally, this relies on the symmetry of the fiber couplers. We require the splitting ratios to be $1/3 : 1/3 : 1/3$, where an input signal at any one of the inputs is equally distributed in the three outputs. We use the same coupler for the interferometers input and output [20], and for both interferometers the coupling ratios are within 5% of this ideal value. We can then observe the three orthogonal states corresponding to the three differ-

ent coincidence detections, $0_A 0_B$, $0_A 1_B$, $0_A 2_B$, or their cyclic permutations. When the phases are varied the coincidences vary as a function of Alice and Bob's phase vectors, a sample of which is inset on the left of Fig. 1 for a fixed but arbitrary ratio of medium and long phases. For more technical details concerning the experimental scheme, we refer the reader to [22].

The CGLMP-Bell inequality is defined in terms of the measurement probabilities, which we can define for these states as $P^{\text{Phase } A, \text{Phase } B}$ (Result A, Result B). Because of the coupler symmetries, we can satisfy the following constraints: $P^{mn}(0, 0) = P^{mn}(1, 1) = P^{mn}(2, 2)$; $P^{mn}(0, 1) = P^{mn}(1, 2) = P^{mn}(2, 0)$; $P^{mn}(2, 1) = P^{mn}(0, 2) = P^{mn}(1, 0)$. These relationships then simplify the inequality such that

$$I_3 = 3[\{P^{11}(0, 0) - P^{11}(0, 1)\} + \{P^{21}(0, 1) - P^{21}(0, 0)\}$$
$$+ \{P^{22}(0, 0) - P^{22}(0, 1)\} + \{P^{12}(0, 0) - P^{12}(0, 2)\}]$$
$$\leq 2 \text{ (for local variables)}. \qquad (2)$$

For this inequality Alice and Bob have a choice of two phase settings each. Each of these settings is a vector of two phases. We define phase vectors, $A_i = (\alpha_{mi}, \alpha_{li})$, for Alice's, and $B_i = (\beta_{mi}, \beta_{li})$, for Bob's. The optimal *Bell* phase vectors are [16,23] $A_1 = (0, 0)$; $A_2 = (\pi/3, 2\pi/3)$; $B_1 = (\pi/6, \pi/3)$; $B_2 = (-\pi/6, -\pi/3)$. The combination of the interferometers and these phases realize a von Neumann measurement that is optimal in complete generality. Here we note that for each of these phase vectors we have the second phase equal to twice the first phase. We see in Eq. (1) that the state's phases depend on the sum of the phases in the two interferometers and one can also see that the vector sum of the Bell phases, $A_1 + B_1$, $A_1 + B_2, \ldots$ etc., retains this relationship which is an important constraint that we will come back to momentarily. With these settings the coincidence probabilities are further constrained such that we have each of the four bracketed terms in Eq. (2) equal. The inequality thus reduces to

$$I_3 = 12[P^{11}(0,0) - P^{11}(0,1)]$$
$$= 12\left[\frac{4 + 2\sqrt{3}}{27} - \frac{1}{27}\right] \approx 2.872\ldots. \qquad (3)$$

We now consider imperfections in the system. The simplest way to do this is to introduce noise to the system, and when looking at Bell inequalities one normally uses a symmetric noise model. One can then characterize the system in terms of its robustness to the admixture of noise. Consider the state

$$\rho = \lambda|\psi\rangle\langle\psi| + (1 - \lambda)\frac{I_9}{9}, \qquad (4)$$

where $|\psi\rangle$ is a maximally entangled pure qutrit state and I_9 is the Identity operator for the entangled qutrit space, $d^2 = 9$. The CGLMP-Bell inequality scales simply with this mixing parameter, λ, such that $I(\rho) = \lambda I_3$ [16]. Inverting this gives the critical mixing value such that the inequality is violated. This inequality is defined for arbitrary finite dimensions and one finds for $d = 2$, $\lambda_2^c = 1/\sqrt{2} \approx 0.707$. For qutrits, $d = 3$, the critical mixing value is lower, $\lambda_3^c = (6\sqrt{3} - 9)/2 \approx 0.696\ldots$ and, hence, it is more robust with respect to noise.

The CGLMP-Bell inequality reveals the robust nature of higher-dimensional entanglement as the amount of noise that can be added to the system increases with the dimensions of the system [16]. It has also been shown that the robustness of the CGLMP-Bell inequality is equivalent for other types of "natural" noise models [24]. For example, choosing a phase noise model, a mixture of the $|ss\rangle$, $|mm\rangle$, and $|ll\rangle$ components, which is quite realistic for energy-time entanglement over tens of kilometers, will produce the same results as in (5) and (6).

If we assume a symmetric noise model as in Eq. (4) for our experiment, then we can determine the coincidence probabilities as a function of the two phases, in the medium and long arms of the two interferometers, and the mixing parameter, λ:

$$P_{jk} \propto 3 + 2\lambda[\cos(\alpha_m + \beta_m + \phi_{jk}^m) + \cos(\alpha_l + \beta_l + \phi_{jk}^l)$$
$$+ \cos(\alpha_m + \beta_m - \alpha_l - \beta_l + \phi_{jk}^m - \phi_{jk}^l)]. \qquad (5)$$

In practice, we do not take measurements at fixed phase settings; instead we continuously scan the phases. This is done in a controlled manner such that we always have the long phase twice that of the medium, as is the case for the Bell phase vectors, as previously mentioned. Hence, the coincidence probability becomes a function of just the one phase and the mixing parameter as in the qubit case. This is confirmed experimentally by looking at the interference events associated with the satellite peaks in the arrival-time histogram. It can be shown that if the phase is varying at the same rate in both of these peaks then we have the desired factor of 2 relating the two phases [22].

This means that we have the symmetry simplified to the level of Eq. (3). It also means that we can use a fitting function based on Eq. (5) to directly determine λ and, hence, also determine the value for the CGLMP-Bell inequality.

We have used interferometric methods to generate entangled qutrits and as such we would like to analyze the system using standard interferometric techniques, such as interference visibilities. This approach is well understood and often used when characterizing qubit schemes. In the case of qubits the mixing parameter, λ, corresponds directly to the visibility and, hence, a visibility greater than λ_2^c implies the state is capable of violating the inequality. Of course, to infer this violation one must be able to satisfy various constraints that depend on the symmetry of the system.

In the case of qutrits, and states of higher dimensions in general, we then can define the visibility in the following manner. Consider Eq. (4), with the identity and the entangled state temporarily defined on a d^2-dimensional space, such that we have the following result:

$$V(d) = \frac{R_{\max} - R_{\min}}{R_{\max} + R_{\min}} = \frac{d\lambda}{2 + \lambda(d - 2)}. \qquad (6)$$

Here one can imagine that for some combination of detectors we have perfect correlations and expect a maximum coincidence rate of $R_{\max} = \lambda + (1 - \lambda)/d$, the first term due to the d possible outcomes and the second term due to the noise. If we are perfectly uncorrelated, we expect $R_{\min} = (1 - \lambda)/d$ due only to the noise. To satisfy these conditions in our experiment, we need the same symmetry constraints on the interferometer couplers and the 2:1 phase constraint, as one needed for the Bell test.

In Fig. 2, we show this function and clearly see that, while the critical values for λ, denoted by (*), to violate the Bell inequality do decrease, marginally, with the dimensions, the visibility becomes significantly more robust. For the case of qutrits we have $V(3) = 3\lambda/(2 + \lambda)$ which implies a visibility greater than $0.775\ldots$, even
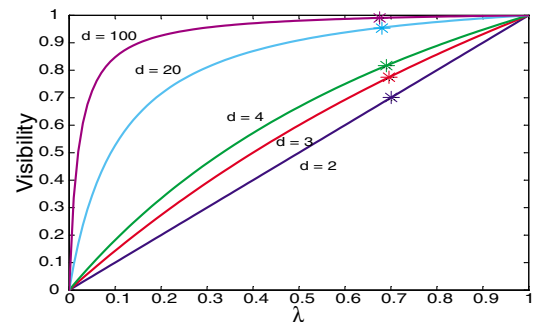

FIG. 2 (color online).   The relationship between the mixing parameter λ and the visibility for various dimensions. Also shown are the critical values for λ (*) to violate the Bell inequality.
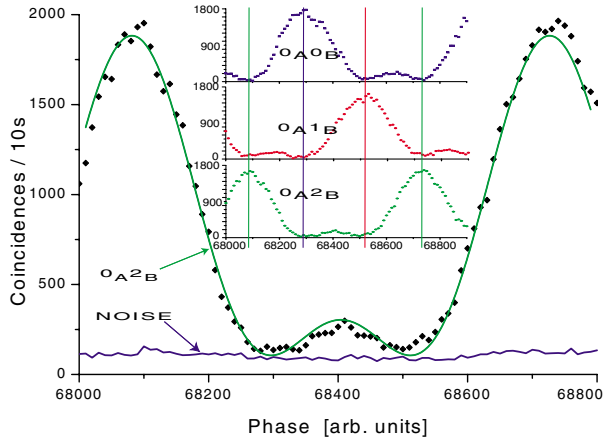
FIG. 3 (color online). Raw coincidence count rates, circles, as the phases are varied under the Bell phase constraint. Also shown is a fit using Eq. (5) and the noise level. Inset: the three (net) orthogonal results.

though we have added more noise than in the qubit case. Experimentally, this can be reconciled, in part, as a result of the standard Bell model and symmetric noise which adds the noise to irrelevant degrees of freedom.

In Fig. 3, we see the coincidence counts as a function of one phase, with the other in this fixed 2:1 relationship. A least-squares fit of this data returns a value $\lambda = 0.848 \pm 0.008$. From this we can then directly calculate the inequality, $I_{exp} = \lambda I_3 = 2.436 \pm 0.023$, which corresponds to a violation of the inequality by 19σ. If, on the other hand, we wish to directly interpret this in terms of the visibility, we can use Eq. (6) and obtain $V(3) = 0.893 \pm 0.006$. The critical visibility value for qutrits is $0.775\ldots$, and we find from the visibility a violation of 19σ as we would expect from the previous result. This is the raw result which includes the background noise counts as well as those due to the correlated photons. We can directly, and concurrently, measure this noise (also shown in Fig. 3) by looking at detection events that arrive outside of these five peaks in the histogram of Fig. 1. If we subtract this noise and look at the net results, we find $\lambda_{net} = 0.969 \pm 0.008$, which in turn gives us a net Bell value of $I_{exp\text{-}net} = \lambda_{net} I_3 = 2.784 \pm 0.023$ and a net visibility of $V(3)_{net} = 0.979 \pm 0.006$ with a violation of the inequality by 34σ.

In the inset of Fig. 3, we have shown the net coincidence counts for the three orthogonal outputs, corresponding to coincidence detections at $0_A 0_B, 0_A 1_B, 0_A 2_B$; the raw results for the curve $0_A 2_B$ are shown in the main figure. We clearly see the signature three-way symmetry for the entangled qutrits with the maxima evenly separated in phase space. In terms of the correlations, we also see that for each maxima for one output we have minima, almost at the noise level, at the other two as we would expect given the high visibility.

In this Letter, we have presented the results for a Bell-type test for energy-time entangled qutrits achieving violations of 19 and 34σ for the raw and net results, respectively. We have also derived a simple means of determining this violation in terms of interference visibility. We have approached both the experimental design and the Bell test itself with the generation and characterization of a source of useful qutrit entanglement in mind. The high signal to noise level for the raw results reinforces the utility of this arrangement and its suitability to high dimensional long distance quantum communication.

*Electronic address: Robert.Thew@physics.unige.ch

[1] J. S. Bell, *Speakable and Unspeakable in Quantum Mechanics* (Cambridge University Press, Cambridge, England, 1964).

[2] A. Zeilinger, Rev. Mod. Phys. **71**, S288 (1999), and references therein.

[3] A. Einstein, B. Podolsky, and N. Rosen, Phys. Rev. **47**, 777 (1935).

[4] A. Acin et al., quant-ph/0310166 [Int. J. Quant. Inf. (to be published)].

[5] C. Brukner, M. Zukowski, and A. Zeilinger, quant-ph/0205080.

[6] H. Bechmann-Pasquinucci and A. Peres, Phys. Rev. Lett. **85**, 3313 (2000).

[7] D. Bruß and C. Macchiavello, Phys. Rev. Lett. **88**, 127901 (2002).

[8] N. J. Cerf et al., Phys. Rev. Lett. **88**, 127902 (2002).

[9] J. C. Howell et al., Phys. Rev. Lett. **88**, 030401 (2002).

[10] A. Vaziri, G. Weihs, and A. Zeilinger, Phys. Rev. Lett. **89**, 240401 (2002).

[11] N. K. Langford et al., quant-ph/0312072.

[12] H. de Riedmatten et al., quant-ph/0309058.

[13] W. Tittel et al., Phys. Rev. A **59**, 4150 (1999).

[14] R. T. Thew et al., Phys. Rev. A **66**, 062304 (2002).

[15] I. Marcikic et al., Nature (London) **421**, 509 (2003).

[16] D. Collins et al., Phys. Rev. Lett. **88**, 040404 (2002).

[17] J. D. Franson, Phys. Rev. Lett. **62**, 2205 (1989).

[18] M. Reck and A. Zeilinger, *Proceedings of the Adriatico Workshop on Quantum Interferometry* (World Scientific, Singapore, 1993), p. 171.

[19] S. Tanzilli et al., Electron. Lett. **37**, 28 (2001).

[20] We have shown Mach-Zender interferometers which are intuitively easier to understand; however, in reality, we use Michelson interferometers which are more practical.

[21] M. Zukowski et al., Phys. Rev. A **55**, 2564 (1997).

[22] R. T. Thew et al., Quant. Inf. Comm. **4**, 93 (2004).

[23] T. Durt, D. Kaszlikowski, and M. Zukowski, quant-ph/0101084.

[24] A. Acín et al., Phys. Rev. A **65**, 052325 (2002).